SAND2013-3189C

Unsteady Shock Motion in a Transonic Flow over a Wall-Mounted Hemisphere

Steven J. Beresh, John F. Henfling, Russell W. Spillers, and Brian O. M. Pruett

1 Introduction

The flow over transonic turrets has been the subject of a number of studies, with primary attention paid to the separated region responsible for most aero-optical distortion [1]. The unsteady effects of shock motion over hemispherical geometries are known but have received little attention. However, shock/boundary layer interactions have been extensively studied at supersonic speeds over other types of aircraft protuberances [e.g., 2-3] and transonically over two-dimensional bumps [e.g., 4-5], which allow inferences concerning the shock behavior on a hemispherical geometry. Recently, the physical sources of the unsteady shock behavior in a variety of these flows have been reviewed [6]. The present work uses Particle Image Velocimetry (PIV) data to study the transonic flow over a wall-mounted hemisphere to compare with the existing body of knowledge concerning shock/boundary layer interactions, focusing on the behavior and origin of this transonic shock motion with a strongly turbulent separated wake.

2 Experimental Approach

Experiments were performed in Sandia's Trisonic Wind Tunnel, which is a blowdown-to-atmosphere facility using air as the test gas through a 305 × 305 mm^2 test section. A hemisphere of radius 38.0 mm was mounted on the top wall, as shown in Fig. 1. It was fabricated from polished acrylic to minimize laser flare and allow measurements near the hemisphere surface. The wall upon which it mounted was made of anodized aluminum and exhibited much greater laser flare, limiting measurements near the wall. Data given herein were acquired at a freestream Mach number of M_∞=0.8 with stagnation pressure P_0=168 kPa. The 99% boundary layer thickness has been measured as 13.4 ± 0.4 mm from earlier PIV data acquired

Sandia National Laboratories · Albuquerque, NM, U.S.A.

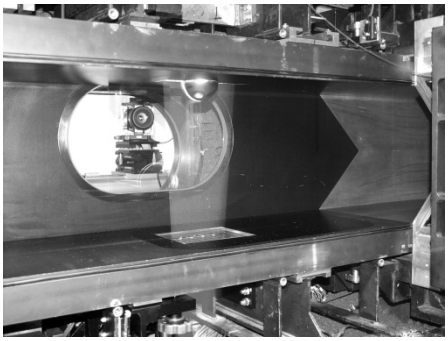

Fig. 1 Photograph of the acrylic hemisphere mounted in the wind tunnel with the laser sheet.

at about the same downstream position as the hemisphere.

The wind tunnel is seeded for PIV by a thermal smoke generator that produces particles from a mineral oil base, which were measured *in situ* to be 0.7 - 0.8 μm diameter. Stokes numbers have been estimated as 0.04 based on *a posteriori* measurements of the hemisphere wake, which is sufficiently small to follow the strongest velocity gradients in the wake.

Two separate experiments were conducted. The light source for both was a frequency-doubled dual-cavity Nd:YAG laser that produced about 400 mJ per beam. A laser sheet 1.2 mm thick was aligned along the spanwise centerline of the hemisphere. In the first experiment, stereoscopic measurements were conducted using two interline-transfer CCD cameras with a resolution of 2048 × 2048 pixels digitized at 8 bits, each using a 200 mm lens mounted for Scheimpflug focusing. The field of view concentrated on the top surface of the hemisphere and its wake, eschewing the incoming boundary layer and hemisphere leading edge. A larger field of view would have compromised the spatial resolution. Images were interrogated using LaVision's DaVis with an initial pass of 64 × 64 pixel interrogation windows, followed by two iterations of 32 × 32 pixel windows.

In a subsequent experiment, the cameras were replaced by CMOS versions with resolution 2560 × 2160 pixels digitized at 16 bits. In this case, each camera independently recorded two-component data. One camera viewed the hemisphere to observe the shock motion while the other was located 80 mm upstream to simultaneously measure the incoming boundary layer. The hemisphere was imaged with a field of view similar to the first experiment, but a 400-mm lens and a shorter standoff distance allowed the boundary layer camera to obtain a much smaller field of view. Since the same laser sheet illuminated the flow seen by both cameras, the typical particle displacement was larger in the boundary layer, but this was easily accounted in the image interrogation. Hemisphere images were interrogated as in the first experiment, whereas the boundary layer images used a first pass of a 128 × 128 pixel window and two iterations at 48 × 48 pixel using 4:1 elliptical Gaussian weighting to align with the dominant vertical velocity gradient.

3 Results and Discussion

Approximately 2000 individual realizations have been acquired for the first, stereoscopic experiment; about 3400 realizations were acquired for the second,

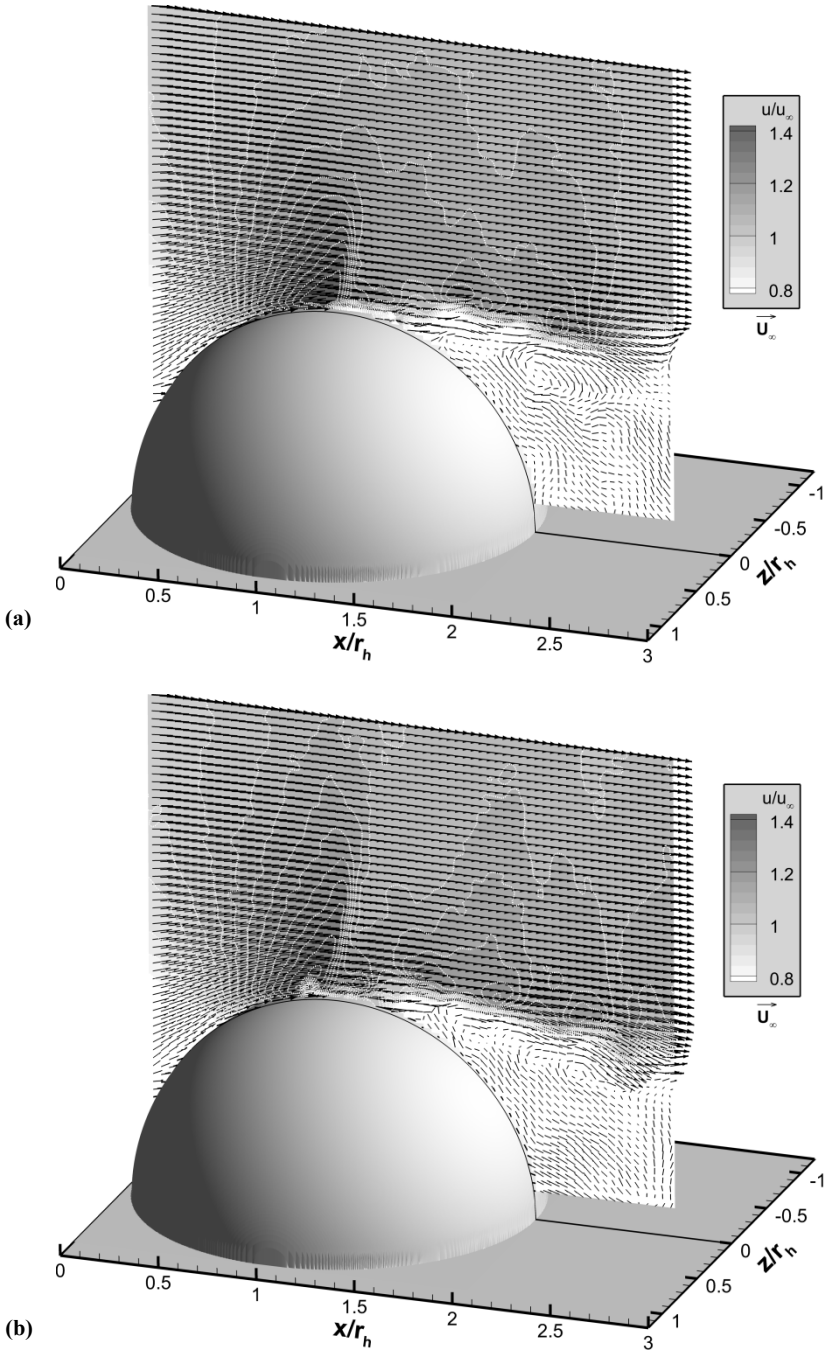

Fig. 2 Two sample instantaneous realizations of the flow, with vectors subsampled 2×2 and contour levels cut off below 0.8.

two-component experiment. Results are normalized to the hemisphere radius r_h and the freestream velocity U_∞. The origin of the coordinate axes was set to the upstream edge of the hemisphere at the wind tunnel floor.

Two examples of instantaneous realizations of the velocity field are given in Fig. 2 based on the stereoscopic data, with velocity vectors superposed on contours of the streamwise velocity u/U_∞. Vectors are subsampled 2 × 2 and contours of u/U_∞ are cut off below 0.8 for improved clarity of the vectors in the wake. The flow can be observed to accelerate over the hemisphere, reaching a peak value just below u/U_∞=1.3. At this point, near the top of the hemisphere, a shock wave forms and initiates separation, from which a strong shear layer and wake grows. Both examples show several large turbulent eddies in the wake accompanied by undulations of the shear layer. A large, strong recirculation region is evident with reverse velocities exceeding u/U_∞=-0.2. Reverse flow moves along the surface of the hemisphere back towards the separation point before recirculating to a positive velocity. Also visible are differing shock positions. Figure 2a shows the shock nearly normal and resting at x/r_h=1.07, slightly downstream of the apex of the hemisphere. Conversely, the shock foot in Fig. 2b sits at x/r_h=0.96, upstream of the hemisphere zenith, and distinctly leans downstream. An examination of all such instantaneous snapshots reveals a range of shock locations near the surface.

To quantify the unsteady shock motion, the location of the shock foot can be found from each instantaneous velocity field and a probability density function of its position can be created. This was accomplished by interpolating velocities onto a circular arc at some radius beyond the hemisphere surface and locating the point at which the velocity begins to rapidly fall. Figure 3 shows the result at multiple heights above the surface. A height of r/r_h=1.05 is as close to the surface as measurements were found to be effective and acts as a surrogate for the shock foot position. These distributions show that the shock foot typically sits just forward of the apex of the hemisphere, though it can move slightly onto the downstream slope. As the shock propagates away from the surface, it shifts downstream then gradually straightens, with the range of motion narrowing.

In an effort to locate a correlation between the wake structure and the shock motion, conditional averages were generated based on the shock foot position as determined by the r/r_h=1.05 data. Two conditional vector fields were created, one representing when the shock foot lay more than one standard deviation upstream of the mean point, and a second for the shock foot more than one standard deviation downstream. These results are given in Fig. 4. Here, the contours represent the total velocity magnitude rather than just the streamwise component. The

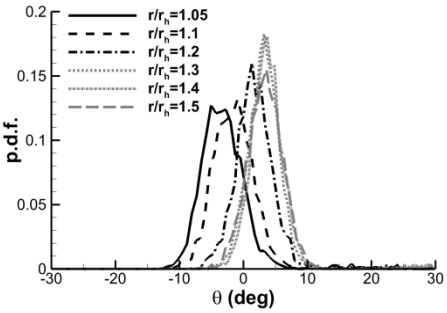

Fig. 3 Probability density functions of the shock location at several heights above the surface.

separation region appears to possess the same structure in each case, but is located at differing positions along the hemisphere surface. More significantly, the magnitudes of the reverse velocities are greater in the upstream shock case, suggesting that stronger reverse flow pushes the shock to an upstream location. However, it is impossible to differentiate cause and effect since the shock position is recorded simultaneously with the wake velocities.

The simultaneous measurements of the incoming boundary layer from the second, two-component experiment were used to seek a correlation between the boundary layer state and the shock position. Similar to Fig. 4, conditional velocity profiles of the boundary layer were generated 65 mm upstream of the hemisphere based upon shock upstream and shock downstream cases, which are given in Fig. 5 along with an average of all boundary layer data. No difference can be identified. Though the boundary layer and shock position are recorded simultaneously, the distance traveled between these points corresponds to roughly 3 kHz. Therefore, a direct influence of the upstream boundary layer upon the shock position, were it to exist, should be detectable since the historical database suggests that in the present

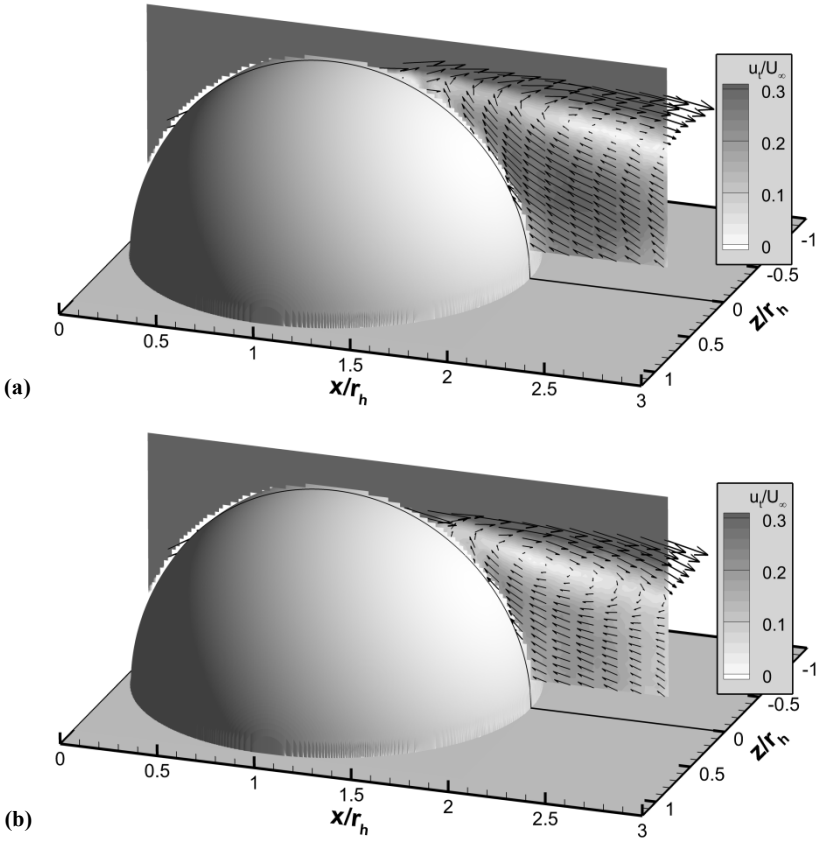

Fig. 4 Conditional averages of the wake for (a) shock upstream and (b) shock downstream cases; contours are given for the total velocity magnitude.

case, low-frequency large-scale shock motion can be expected approximately an order of magnitude lower [2, 3].

4 Conclusions

The current measurements show that the position of the transonic separation shock on the hemisphere surface moves upstream when the reverse velocities in the recirculation region are strong and is located downstream when they are weaker. No correlation was detected between the incoming boundary layer and the shock position. These observations are consistent with recent studies concluding that for large strong separation regions, the dominant mechanism is the instability of the separated flow rather than a direct influence of the incoming boundary layer [6, 7]. However, it is possible that the upstream boundary layer influences the shock position by affecting the shear layer instability at separation, which would not be captured by the present experiment if the response time is lengthy.

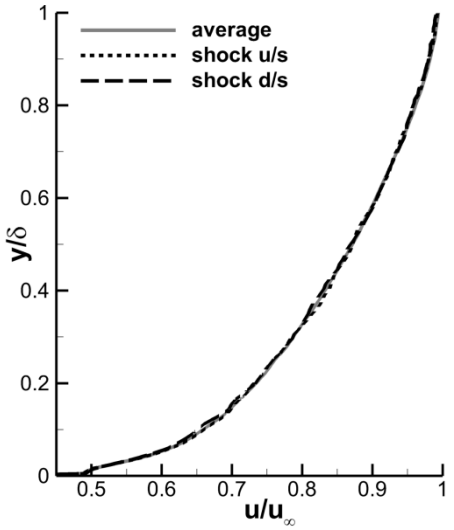

Fig. 5 Conditional velocity profiles of the incoming boundary layer based on different shock positions.

References

1. Gordeyev S., and Jumper, E.: Fluid Dynamics and Aero-Optics of Turrets, Progress in Aerospace Sciences, 46 (8), 388-400, (2010)
2. Smits A. J., and Dussauge, J.-P..: *Turbulent Shear Layers in Supersonic Flow*, 2nd ed. (Springer, 2006), 319-363
3. Dolling D. S.: Fifty Years of Shock-Wave/Boundary-Layer Interaction Research: What Next?, AIAA Journal, 39 (8), 1517-1531, (2001)
4. Delery J. M.: Experimental Investigation of Turbulence Properties in Transonic Shock/Boundary-Layer Interactions, AIAA Journal, 21 (2), 180-185, (1983)
5. Liu X., and Squire L. C.: An Investigation of Shock/Boundary-Layer Interactions on Curved Surfaces at Transonic Speeds, Journal of Fluid Mechanics, 187, 467-486, (1988)
6. Clemens N. T., and Narayanaswamy, V..: Shock/Turbulent Boundary Layer Interactions: Review of Recent Work on Sources of Unsteadiness, AIAA Paper 2009-3710, (2009)
7. Souverein L. J., Dupont P., Debieve J.-F., Dussauge J.-P., van Oudheusden B. W., and Scarano F.: Effect of Interaction Strength on Unsteadiness in Turbulent Shock-Wave-Induced Separations, AIAA Journal, 48 (7), 1480-1493, 2010.